

# X-ray Diffraction in the Multimegabar Regime Using Synchrotron Radiation at the Cornell High-Energy Synchrotron Source (CHESS)

ARTHUR L. RUOFF

Department of Materials Science, Cornell University, Ithaca, New York 14853

Received October 20, 1987 (Revised Manuscript Received March 16, 1988)

The development of the diamond anvil cell for generating high pressures has heralded a new era for high-pressure research. It is now possible to generate multimegabar static pressures with the diamond anvil cell and to perform optical and X-ray diffraction measurements on pressurized samples. Jayaraman has reviewed the diamond anvil cell<sup>1</sup> and its applications in a number of areas.<sup>2</sup> At multimegabar pressures the sample volume becomes tiny ( $10^{-10}$  cm<sup>3</sup>) so that powerful sources and detection techniques have to be employed. Substantial progress in X-ray diffraction has been made possible by combining the diamond anvil cell with the Cornell High-Energy Synchrotron Source (CHESS). Our group has used CHESS to obtain significant X-ray diffraction results on several important materials, often combining the X-ray studies with optical absorption and reflectivity measurements,<sup>3</sup> Raman spectroscopy,<sup>4</sup> and electrical resistivity measurements.<sup>5</sup> Phenomena studied include structural transitions in insulators, semiconductors, and metals, equation of state studies, and band gap closure of (initially) electrical insulators and critical parameters associated with multimegabar generation and experimentation in the diamond cell.

In this paper we focus on the application of the energy-dispersive X-ray diffraction (EDXD) technique. We show that excellent X-ray diffraction patterns can be obtained, even above 200 GPa (2 Mbar). In general we describe experiments of high difficulty at this time, but we wish to point out that similar experiments on a wide array of materials at somewhat lower pressure (20 and even 40 GPa) are relatively routine. The reader should also be aware that a National High-Pressure Beam Line Facility is being established at CHESS. This will be a fully instrumented facility, and outside investigators need bring only their diamond cells. We expect this facility, when it is completed in 1990, to have the capability of working with angle-dispersive as well as energy-dispersive techniques and with single crystals as well as polycrystalline samples.

Figure 1a shows a schematic of how diamond anvils are arranged within a diamond anvil cell. A convenient

starting point for producing a diamond anvil is choosing an extremely high quality one-third carat brilliant cut gemstone. This stone is modified to have 16 side facets. The culet (the sharp tip) is then polished away to produce either a flat tip (with 16 sides) or a beveled tip with a central flat with typically a "radius" of 25  $\mu$ m followed by a bevel with an angle of 7° out to a "radius" of 150  $\mu$ m.<sup>6</sup> There are backup plates which are caused to push on the diamonds; these plates have slits in them to allow the incident beam to enter and the diffracted beam to leave. The diamond anvil cell has mechanisms that can move the diamonds laterally so their tips are aligned and a mechanism so the flats of the tips can be made parallel to each other (by observing Newton's rings).<sup>7</sup> The gasket begins as a sheet of stainless steel, spring steel, or rhenium. This sheet is placed between the anvils, and a force is applied that preindents the anvils. The gasket is then removed, and the sample hole, as small as 12  $\mu$ m in diameter, is drilled with a carbide drill.<sup>8</sup> A convenient way to measure pressure is to mix with the sample a marker material (such as Fe, Au, or Pt) whose equation of state is known from shock data and to measure the lattice parameters of the marker material (assuming the peaks of the marker material are distinct from the peaks of the sample). The pressure can then be calculated from the known *P-V* relationship. This is known as the marker method of determining pressure.

It is useful to have a perspective on the pressures and dimensions used here. The pressure of 1 bar is 98% of an atmosphere of pressure. City water pressure is a few bars, the pressure at the deepest spot in the ocean (about 35 000 ft) is about 1 kbar (0.1 GPa), and the pressure at the center of the earth is 3.5 Mbar (350 GPa). A convenient reference for the diamond tip diameter and the sample diameter is a human hair diameter, which is about 75  $\mu$ m.

In energy-dispersive X-ray diffraction (EDXD) a polychromatic X-ray beam is diffracted from a polycrystalline sample, with the diffracted X-rays entering a slit at a *fixed angle* in front of a solid-state detector.

Arthur L. Ruoff has been the Director of the Department of Materials Science and Engineering at Cornell University since 1978. During his tenure in this position, he created MS&E News and the MS&E Industrial Affiliates program, and he dramatically helped to increase enrollment in MS&E at both the undergraduate and graduate levels. He also served as Program Committee Chairman of the National Research and Resource Facility for Submicron Structures (now the Nanofabrication Facility) for several years. He is the author of two books in materials science, an audiotutorial course in Elements of Materials Science, and over 190 research publications. His research interest is the study of solids at extreme pressures (measured in megabars), and he is an expert in X-ray diffraction at high pressure. He is a Fellow of the American Physical Society and a member of the Executive Committee of AIRAPT, the International association for high-pressure research.

- (1) Jayaraman, A. *Rev. Sci. Instrum.* 1986, 57, 1013.
- (2) Jayaraman, A. *Rev. Mod. Phys.* 1983, 55, 65.
- (3) Vohra, Y. K. *Scr. Metall.* 1988, 22, 145.
- (4) Hemley, R. J.; Porter, R. F. *Scr. Metall.* 1988, 22, 139.
- (5) Weir, S. T.; Ruoff, A. L. *Scr. Metall.* 1988, 22, 151.
- (6) The only known source (to the author) of 16-sided beveled diamonds is Dubbledde Diamond Corp., 100 Sterli Court, Mt. Arlington, NJ 07856.
- (7) Baublitz, M. A.; Arnold, V.; Ruoff, A. L. *Rev. Sci. Instrum.* 1981, 52, 1616.
- (8) These holes are drilled with carbide drills mounted in mandrels that rotate in grooved diamonds in a special drill press invented by John Cupler, National Jet Co., 10 Cupler Drive, Lavale, MD 21602.

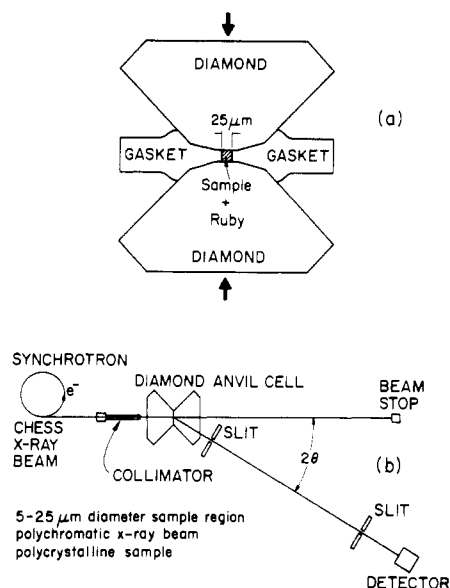


**Figure 1.** (a) Schematic of diamonds and gasket in a diamond anvil cell. (b) Schematic of energy-dispersive X-ray diffraction setup (with different items on vastly different scales). The collimator can be moved by  $\pm 1.0 \mu\text{m}$  in two perpendicular directions and tilted about independent axes.

**Table I**  
Photon Flux through a 10- $\mu\text{m}$ -Diameter Collimator at CHES Operating at 5.3 GeV and 100 mA<sup>a</sup>

energy, keV	CHES	
	bending magnet	wiggler
30	120	1300
40	64	1300
50	32	1200
60	14	880

<sup>a</sup>The units are  $10^6$  photons/s-1% bandwidth (10- $\mu\text{m}$ -diameter collimator).

The experimental configuration is shown schematically in Figure 1b. For EDXD studies, Bragg's law is

$$Ed = hc/2 \sin \theta = \text{constant} \quad (1)$$

Here,  $E$  is the peak energy,  $d$  is the interplanar spacing,  $h$  is Planck's constant,  $c$  is the speed of light, and  $\theta$  is the Bragg angle.

A spectrum consists of intensity versus energy obtained with the use of a solid-state intrinsic germanium detector and a multichannel analyzer. The Cornell High-Energy Synchrotron Source (CHES) supplies the X-rays. An essential feature is the slits on the downstream side of the pressure vessel, which prevent most of the Compton-scattered X-rays (primarily from the downstream diamond) from reaching the detector. A pinhole collimator is located in front of the diamonds and extends into the pressure cell, nearly reaching the backup plate of the first diamond. This collimator can be tilted and also can be moved in two perpendicular directions normal to the beam in 1- $\mu\text{m}$  increments. Details of our use of EDXD with the diamond anvil cell (DAC) are described elsewhere.<sup>7,9</sup> Table I illustrates the magnitude of the photon fluxes at the high energy obtainable at CHES.<sup>10</sup> These CHES beams provide

(9) Brister, K. E.; Vohra, Y. K.; Ruoff, A. L. *Rev. Sci. Instrum.* 1986, 57, 256.

(10) Ruoff, A. L.; Vohra, Y. K.; Bassett, W. A.; Batterman, B. W.; Bilderback, D. H. *J. Nucl. Instrum. Methods Phys. Res. A* 1988, 266, 344.

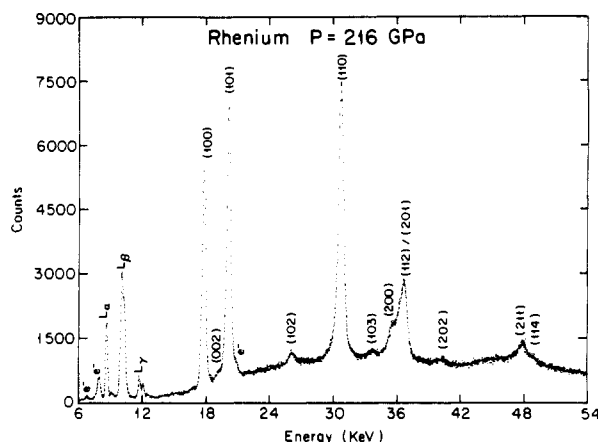


**Figure 2.** Diffraction pattern of rhenium at 216 GPa using the beam from the CHES bending magnet. Here  $\theta = 9.311^\circ$ . The beam was collimated to a diameter of 10  $\mu\text{m}$ , and the data collection time was 90 min. Here e<sup>-</sup> represents an escape peak from the detector and the L's represent fluorescence peaks.

**Table II**  
Comparison of Observed and Calculated Interplanar Spacings for Rhenium at 216 GPa ( $V/V_0 = 0.734$ )<sup>a</sup>

hkl	$d_{\text{obsd}}$ , Å	$d_{\text{calcd}}$ , Å	$(d_{\text{obsd}} - d_{\text{calcd}})/d_{\text{obsd}}$
100	2.154	2.157	-0.0014
002	2.004	2.010	0.0030
101	1.901	1.901	0
102	1.468	1.471	-0.0020
110	1.246	1.246	0
103	1.139	1.138	0.0009
200	1.078	1.079	-0.0009
112	1.056	1.059	-0.0028
201	1.043	1.042	-0.0010
202	0.9506	0.9504	0.0002
211	0.7996	0.7991	0.0006
114	0.7831	0.7821	0.0013

<sup>a</sup>The calculated interplanar spacings ( $d$ ) are based on the fitted parameters for the hexagonal closest packed structure of  $a = 2.491 \pm 0.003$  Å,  $c = 4.020 \pm 0.005$  Å, and  $c/a = 1.614 \pm 0.004$ . The excellent quality of diffraction data at this pressure is indicated by the small fractional deviation of the calculated line positions from those observed.

the highest photon fluxes available at high energies in the world today.

## Results

Figure 2 shows an X-ray diffraction pattern of rhenium obtained with a 10- $\mu\text{m}$ -diameter collimated beam at 216 GPa (2.16 Mbar).<sup>11</sup> The sample volume is about  $10^{-10} \text{ cm}^3$ . In this case no sample hole was present in the gasket. The pressure was measured by using the measured lattice parameter along with the experimental equation of state (to 300 GPa) obtained from shock data.<sup>9</sup> In fact all pressure measurements above 7.4 GPa depend on X-ray measurement of lattice parameters of a material whose equation of state is determined by shock methods. Secondary standards such as the ruby scale<sup>13</sup> depend on the marker method for calibration.<sup>14</sup> Table II lists the measured interplanar spacings for the

(11) Vohra, Y. K.; Duclos, S. J.; Ruoff, A. L. *Phys. Rev. B* 1987, 36, 9790.

(12) McQueen, R. G.; Marsh, S. P.; Taylor, J. W.; Fritz, J. N.; Carter, W. J. In *High Velocity Impact Phenomena*; Kinslow, R., Ed.; Academic: New York, 1970; p 293.

(13) Barnett, J. D.; Block, S.; Piermarini, G. J. *Rev. Sci. Instrum.* 1973, 44, 1.

(14) Mao, H. K.; Bell, P. M.; Shaner, J. W.; Steinberg, D. J. *J. Appl. Phys.* 1978, 49, 3276.

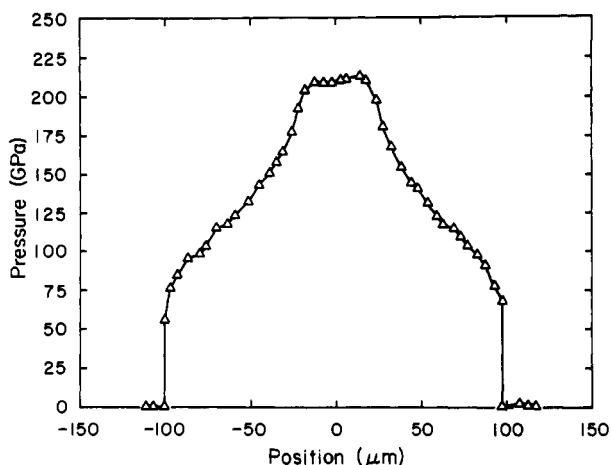


**Figure 3.** Pressure profile in a rhenium gasket (without a sample hole) across a diameter of the diamond anvils obtained by measuring the lattice parameters and using the known equation of state of rhenium (from shock data). The beam diameter was 5  $\mu\text{m}$ . The tip was flat out to a radius of 25  $\mu\text{m}$  and then had a 7° bevel to 100  $\mu\text{m}$ .

data of Figure 2 and compares these with the values calculated from the fitted lattice parameter. Note that the volume fraction is reduced to 0.734 for rhenium at 216 GPa, the most incompressible of all the elemental metals. This corresponds to a decrease of 9.79% in the lattice parameter. Other more compressible solids such as CsI and xenon would show very much larger reductions in interatomic distances at such pressures. There were two reasons for studying rhenium. First, it had been suggested that a crystalline phase transition may occur in the neighborhood of 1 Mbar.<sup>15</sup> Second, it is an excellent candidate for a gasket material. On the basis of studies of various transition-metal alloys, including rhenium, Mo-Re, Nb-Re, and Ta-Re, Kaufman estimated the difference in the Gibbs free energies (by extrapolation) for the pure hcp and bcc phases in rhenium and on this basis speculated that hcp rhenium might transform to the bcc phase at high pressure. No phase transition was found; moreover, the  $c/a$  ratio for rhenium (which has an hcp crystal structure) remains constant at 1.614 in the pressure range 0–216 GPa.<sup>11</sup>

Rhenium is a potentially good gasket material because of its high stiffness, high flow stress, and high rate of strain hardening. The collimated beam can be moved to overlap the boundary between the gasket and sample (which in general, but not always, will be a softer material); in this way the gasket itself can be used as a marker material, assuming the beam diameter is small compared to the sample diameter. In fact, since the  $c/a$  ratio does not vary with pressure and because peaks in hcp crystals only broaden (but do not have their centroids changed) due to the presence of deformation faults,<sup>16</sup> a single peak of the hcp rhenium can be used to obtain the pressure, unlike the situation for fcc markers such as Au.<sup>16</sup> The experiments on rhenium were obtained with the beam from the bending magnet at CHESS.

We have used X-ray diffraction to obtain the pressure profile across a diamond tip by measuring the lattice parameters of rhenium with a collimated beam having

(15) Kaufman, L. In *Phase Stability in Metals and Alloys*; Rudman, P. S., Stringer, J., Jaffee, R. I., Eds.; McGraw-Hill: New York, 1967.

(16) Barrett, C. S.; Massalski, T. B. *The Structure of Metals*; McGraw-Hill: New York, 1966; p 459.

**Table III**  
Comparison of Some of Our Experimental Transition Pressures with Calculated Phase Transition Pressures

material	nature of transition	exptl, GPa	ref for expt	calcd, GPa	ref for calculations
InAs	zinc blende to sodium chloride	7.0	19	7.8	20
	sodium chloride to $\beta$ -Sn analogue	17.0	19	8.4 19.5	21 20
GaSb	$\beta$ -Sn analogue to disordered simple hexagonal	26.4 $\pm$ 2.6	22	52.8 <sup>a</sup>	21
Si	hcp to fcc	78 $\pm$ 3	23	80 76 116	24 24 25
Ge	$\beta$ -Sn analogue to primitive hexagonal	74	26	84	26
	primitive hexagonal to dhcp	102	26	105 <sup>b</sup>	26

<sup>a</sup>The calculations are for the ordered hexagonal structures with six unlike and two like nearest neighbors. <sup>b</sup>The calculations show that the hcp phase has a lower free energy than the double hexagonal closest packed (dhcp) phase found experimentally.

a diameter of only 5  $\mu\text{m}$  and using these parameters to determine the pressure. The collimated beam could be moved in 1.0- $\mu\text{m}$  increments. A profile along one diameter is shown in Figure 3 for a case in which the maximum pressure is 212 GPa. Altogether, pressure measurements were made at 300 points between and slightly beyond the tips at this loading. Note that data on rhenium were obtained between 80 and 212 GPa at a single load (force on the diamond). The pattern at 212 GPa had 13 well-defined peaks. Such profiles have been obtained with diamonds with bevels of 5°, 7°, and 10°, in an attempt to develop rules for optimizing diamond anvil design.<sup>17</sup>

The reader might ask: why make the collimators so small, since this obviously increases the data collection time? There are two good reasons. First of all, the pressure gradients can be very large (even in the region of the flat part of the diamond, at lower pressures than shown in Figure 3); hence a tiny collimator is needed to provide a nearly constant pressure region. Second, in order to reach still higher pressures, scientists are moving to smaller and smaller tips.<sup>18</sup> Suffice it to say that, if the tip is small enough and the dislocation density low enough, the strength of perfect crystalline diamond can be achieved and higher pressure can be attained.

### Group IVB Elements and III-V Compounds

Recent experimental and theoretical results on these materials<sup>19–26</sup> provide a convenient test of detailed first-principle quantum mechanical calculations of

(17) Brister, K. E.; Vohra, Y. K.; Ruoff, A. L. *Rev. Sci. Instrum.* 1988, 59, 318.

(18) Ruoff, A. L.; Weir, S. T.; Brister, K. E.; Vohra, Y. K. *J. Mater. Res.* 1987, 2, 614.

(19) Vohra, Y. K.; Weir, S. T.; Ruoff, A. L. *Phys. Rev. B* 1985, 31, 7344.

(20) Christensen, N. E. *Phys. Rev. B* 1986, 33, 5096.

(21) Zhang, S. B.; Cohen, M. L. *Phys. Rev. B* 1987, 35, 7604.

(22) Weir, S. T.; Vohra, Y. K.; Ruoff, A. L. *Phys. Rev. B* 1987, 36, 4543.

(23) Duclos, S. J.; Vohra, Y. K.; Ruoff, A. L. *Phys. Rev. Lett.* 1987, 58, 775.

(24) McMahan, A. K.; Moriarty, J. A. *Phys. Rev. B* 1983, 27, 3235.

(25) Chang, K. J.; Cohen, M. L. *Phys. Rev. B* 1985, 31, 7819.

(26) Vohra, Y. K.; Brister, K. E.; Desgreniers, S.; Ruoff, A. L.; Chang, K. J.; Cohen, M. L. *Phys. Rev. Lett.* 1986, 56, 1944.

binding energies and phase transition pressures. Examples are shown in Table III. In the calculations the energy per atom (molecule) is computed as a function of volume for the original structure and for an assumed structure. The negative of the common tangent gives the transition pressure; these are 0 K calculations. It is necessary to assume a number of product structures (possibly missing the correct one) in these procedures. The calculations and experiments are proceeding in parallel, with sometimes one occurring first and sometimes the other.

In the case of InAs, the experiments came first<sup>19</sup> and were followed by two independent calculations<sup>20,21</sup> for the first transition from the zinc blende structure (a fcc lattice with a basis of In at 000 and As at  $1/4, 1/4, 1/4$ ) with a coordination number (CN) of 4 to the sodium chloride structure with a coordination number of 6. There was also one calculation<sup>20</sup> for the next transition to the  $\beta$ -Sn analogue (a body-centered tetragonal lattice plus a basis of In at 000 and As at  $0, 1/2, 1/4$ ), which has approximately six nearest neighbors. In fact at a pressure of 25.2 GPa, the  $c/a$  ratio of the tetragonal crystal equals the ideal ratio of 0.516, for which each atom has exactly six nearest neighbors, four like and two unlike atoms. We note that a rather large 17% reduction in volume occurs at the transition from the semiconducting zinc blende structure (CN = 4) to the metallic sodium chloride structure (CN = 6). The InAs bond length actually increased by 8.5% during this transition and is 5.5% longer than it was at zero pressure in the zinc blende structure. Within experimental accuracy there is no discernible volume change for InAs in the metal-to-metal transition, from the sodium chloride structure (six unlike nearest neighbors) to the  $\beta$ -Sn analogue structure (four unlike and two like approximately nearest neighbors).

The second example in Table III involves GaSb. Here we have not included results at lower pressures, which are reviewed in ref 22. At atmospheric pressure GaSb is a semiconductor with the zinc blende structure, and it transforms at about 6.2 GPa to a metal with the  $\beta$ -Sn analogue structure. Subsequent ab initio pseudopotential calculations gave 6.3 GPa for this transition.<sup>21</sup> These same calculations were extended to higher pressures and correctly predicted that the next phase transition would be to a hexagonal structure. Note that the coordination number is 8 in the ideal case for a  $c/a$  ratio of 1. The actual  $c/a$  ratio is 0.92 for GaSb. The calculations were based on an ordered arrangement with six unlike and two like nearest neighbors. Ordered structures in which an atom has four like and four unlike neighbors or two unlike and six like neighbors were also considered in the calculations but had higher energies. Another structure would have 50% probability that any site on the hexagonal lattice is occupied by a Ga atom (or an Sb atom). This is a disordered simple hexagonal structure. For a discussion of order-disorder phenomena, see ref 27. Table IV shows that the experimental data are consistent with such a disordered hexagonal structure. For the procedure used in calculating the relative intensities in Table IV, see ref 7. We note that there is a disagreement between theory and experiment by a factor of 2 for the transition pressure to the hexagonal phase.

**Table IV**  
Comparison of Calculated and Experimental Interplanar Spacings and Intensities of GaSb in the (Disordered) Simple Hexagonal Type Structure at 56.6 GPa<sup>a</sup>

<i>hkl</i>	$d_{\text{obsd}}$ , Å	$d_{\text{calcd}}$ , Å	rel intensity	
			obsd	calcd
001	2.468	2.479	33.2	18.0
100	2.336	2.336	64.7	57.9
101	1.702	1.700	100.0	100.0
110	1.348	1.349	30.5	27.9
002	1.240	1.240	4.9	6.8
111 + 200	1.185	1.185, 1.168	61.5	47.2

<sup>a</sup>The lattice parameters used are  $a = 2.6981$  and  $c = 2.4790$  Å. The calculated relative intensities were obtained by the procedure described in ref 7. A sample thickness of 20  $\mu\text{m}$  was used.

In the case of Si (Table III) all the calculations of the hcp to fcc transition preceded the experiment, with the generalized pseudopotential method (GPT) yielding 80 GPa, the linear muffin tin orbital method (LMTO) giving 76 GPa, and the ab initio pseudopotential (AP) method yielding 116 GPa. Subsequent to the experimental results quoted in ref 23, we carried out another experiment, using ruby to measure the pressure and loading and unloading in small pressure increments through 78 GPa. We found that the transformation began at 78.5 GPa on loading and that the reverse transformation (from the fully fcc phase) began at 77.5 GPa. It should be emphasized that there is not much difference between the free energies of the hcp and the fcc phase; the nearest-neighbor environment is identical (for the ideal ratio,  $c/a = 1.633$  for closest packed layers of spheres). In fact  $c/a = 1.69$  at 50 GPa and probably decreases to 1.67 at 75 GPa. Thus the calculations have to be quite accurate to even predict that this transition will occur. From an experimental viewpoint, doing EDXD studies on silicon to 100 GPa is not an easy matter because silicon is a low atomic number material and hence has a low atomic scattering factor.

Silicon also undergoes other transitions, and these are reviewed in ref 23. It transforms from a semiconductor with the zinc blende structure (CN = 4) to a metal with the  $\beta$ -Sn structure (CN = 6) at 11 GPa, to a simple hexagonal structure (CN = 8) at 13–16 GPa, to an intermediate unknown structure at 34 GPa, and finally to the hexagonal closest packed structure (CN = 12) above 40 GPa. These pressures have been calculated by AP methods<sup>25</sup> and are in reasonably good agreement with the transition between known phases except theory has not so far helped to identify the intermediate phase. The interatomic distance in the fcc phase is 2.38 Å at 78 GPa, while for the zinc blende phase at atmospheric pressure it is 2.35 Å. There is a prediction of another phase transition in silicon from fcc to bcc in the pressure range 250–360 GPa,<sup>24</sup> a range that is just beyond present capabilities.

Germanium has now been studied to 160 GPa. The transformation from the  $\beta$ -Sn structure to the simple hexagonal structure (see Table III) was studied independently and simultaneously by experiment and by AP calculations, and the results were subsequently published jointly. The agreement is good. The calculations also showed a subsequent transformation to the hcp structure at 105 GPa, while experimentally a transformation instead to the double hexagonal close packed structure (dhcp) was found; the latter has a stacking sequence of closest packed layers of ...

(27) See ref. 16, p 273.

Table V

Phase Transition Pressures and Maximum Pressures to Which the Equation of State of BaX Compounds Have Been Obtained (in GPa)

compd	transition	$P_t$	$P_{max}$	ref
BaO	NaCl to NiAs	10.0	65	31
BaO	NiAs to $PH_4I$	15.0	65	31
BaS	NaCl to CsCl	6.5	89	31
BaSe	NaCl to CsCl	6.0	61	32
BaTe	NaCl to CsCl	4.8	41	33

ABAC...<sup>26</sup> The experimental  $c/a$  ratio for the  $\beta$ -Sn phase is constant ( $0.550 \pm 0.008$ ) on the complete range of its stability, and the calculated value is in excellent agreement. In the simple hexagonal (sh) phase the experimental  $c/a = 0.930 \pm 0.007$ , which is in fair agreement with the theoretical value of 0.945. Finally, for the dhcp phase  $c/2a = 1.681$ , which is somewhat larger than the ideal ratio of 1.633 for a rigid-sphere model.

To complete the story of the group IVB elements with the diamond cubic structure, first-principle calculations show a transformation in diamonds at 800 GPa to a BC8 structure.<sup>28</sup> Perhaps this will set the limit to the pressures attainable in the diamond anvil cell.

### Barium Chalcogenides

We began our studies on the barium chalcogenides as a study on closed-shell systems by considering the isoelectronic series xenon, cesium iodide, and barium telluride, assuming the compounds are fully ionic. This was part of a study to look into possible metalization of these electrical insulators. Since BaTe had the smallest band gap, we studied it first. There is available a simple concept of metalization that predicts metalization at a volume fraction  $V_M/V_0$ . This is the Goldhammer-Herzfeld criterion<sup>29,30</sup>

$$V_M/V_0 = (n_0^2 - 1)/(n_0^2 + 2) \quad (2)$$

Here,  $n_0$  is the refractive index at zero pressure. This follows directly from the Clausius-Mossotti equation (combined with the Maxwell relation) if the assumption is made that the molar refraction does not vary with pressure (or volume) and it is noted that the refractive index  $n$  approaches infinity as metalization is approached. It was therefore clear that if band gap closure was studied as a function of pressure by optical and electrical methods, we should also have a  $P$ - $V$  relationship so that the results could be related to the more fundamental quantity, volume ( $V$ ), and hence to the interatomic spacing. We therefore embarked on an X-ray diffraction study as a function of pressure on the barium chalcogenides. A summary of the results obtained at CHESS is shown in Table V.<sup>31-33</sup>

BaS, BaSe, and BaTe all show an increase in coordination number from 6 to 8 and equations of state were

(28) Biswas, R.; Martin, R. M.; Needs, R. J.; Nielsen, O. H. *Phys. Rev. B* 1984, 30, 3210. Yin, M. T. *Phys. Rev. B* 1984, 30, 1773.

(29) Goldhammer, D. A. *Dispersion and Absorption des Lichtes*; Tubner Verlag: Leipzig, 1913; p 27.

(30) Herzfeld, K. *Phys. Rev.* 1927, 29, 701.

(31) Weir, S. T.; Vohra, Y. K.; Ruoff, A. L. *Phys. Rev. B* 1986, 33, 4221.

(32) Ruoff, A. L.; Grzybowski, T. A. In *Solid State Physics under Pressure*; Minomura, S., Ed.; KTK Scientific Publishers: Tokyo, Japan, 1985; p 69.

(33) Grzybowski, T. A.; Ruoff, A. L. *Phys. Rev. Lett* 1984, 53, 489.

Table VI  
 $V_M/V_0$  Values at Which Metalization Is Found<sup>a</sup>

material	optical measd	resistivity measd	dielectric model	ref
BaS	0.52 <sup>b</sup> (80)		0.55	34
BaSe	0.55 <sup>c</sup> (52)	0.56	0.58	34
BaTe	0.62 <sup>b</sup> (25)	0.63	0.62	33, 35

<sup>a</sup>The corresponding experimental pressures (in GPa) are shown in parentheses. <sup>b</sup>Involves extrapolation of optical absorption edge versus pressure data to zero energy. <sup>c</sup>Involves extrapolation of optical absorption edge versus pressure data to zero and optical reflectivity studies.

Table VII

Phase Transition (in GPa) in the Cesium Halides Studied at CHESS and Comparison with the Zero-Pressure Bulk Modulus  $B_0$

material <sup>a</sup>	$P_t$		$3.5B_0$	$P_{max}$	ref
	CsCl struct to tetragonal	AuCuI struct			
CsCl	65		59	80	40
CsBr	53		50	71.5	40, 41
CsI	39		42	95	36, 39

material	tetragonal to orthorhombic	$P_{max}$	ref
CsI	56 <sup>b</sup>	89	39

<sup>a</sup>For CsCl structure  $\rightarrow$  AuCuI structure for the cesium halides studied,  $(V/V_0)/0.54$ . <sup>b</sup>10-Fold coordinated; eight unlike, two like.

obtained for all of these to pressures higher than the expected metalization pressures. BaO, however, exhibits different behavior, not too surprising since we expect perversity from elements in the second row of the periodic table. Here the coordination number does not change but the nature of the coordination does. In the NaCl structure each atom is octahedrally coordinated with the other. For BaO in the NiAs structure, the barium is at the center of a triangular prism while the oxygen is at the center of a triangular antiprism. The NiAs crystal structure consists of a hexagonal lattice with a basis of oxygen atoms at 000 and  $0,0,1/2$  and barium atoms at  $1/2,0,1/2 + \Delta$  and  $0,1/2,1/2 - \Delta$ . The tetragonal  $PH_4I$  structure has space group  $p4/nmm$  with two ion pairs per unit cell, oxygen atoms at 000 and  $1/2,1/2,0$ , and barium atoms at  $1/2,0,1/2 + \Delta$  and  $0,1/2,1/2 - \Delta$ . If the atomic position parameter  $\Delta = 0$  and  $c/a = 1/\sqrt{2}$ , the structure is the cesium chloride structure. At 60.5 GPa,  $c/a = 0.731$ ,  $\Delta = 0.06$ , and both are decreasing, suggesting the possibility that at higher pressure, perhaps at 150-200 GPa, BaO, like the other barium chalcogenides, will have the cesium chloride structure.

BaTe was the first of the closed-shell systems (rare-gas solids, the alkali halides, and the alkaline chalcogenides) to be metalized.<sup>33</sup> Table VI summarizes the experimental situation<sup>33-35</sup> and compares the results with the Goldhammer-Herzfeld criterion (also called the dielectric model). The agreement is surprisingly good for such a simple model. For barium oxide, the dielectric model gives  $V_M/V_0 = 0.493$ , which corresponds to a pressure of 150 GPa based on extrapolation of our fitted equation of state for BaO in the  $PH_4I$  structure.<sup>31</sup> However, based on the direction of the deviations from the dielectric model (see Table VI) it

(34) Weir, S. T.; Vohra, Y. K.; Ruoff, A. L. *Phys. Rev. B* 1987, 35, 874.

(35) Syassen, K.; Christensen, N. E.; Winzen, H.; Fischer, K.; Evers, J. *Phys. Rev. B* 1987, 35, 4052.

is likely that the volume would be lower and the pressure higher, probably around 200 GPa.

### Cesium Halides

We began our studies with CsI to obtain an equation of state to relate to optical studies of band gap closure. Along the way we found a transition from the cesium chloride structure (CN = 8) to a tetragonal distortion of that structure<sup>36</sup> (the AuCuI structure<sup>27</sup>), which was found simultaneously and independently by others.<sup>37,38</sup> We therefore extended our studies to other cesium halides.<sup>39-41</sup> The results are shown in Table VII. CsBr was also studied by others.<sup>42</sup> This transformation had been anticipated on the basis of a simple Born-Mayer model, which had been used to show that the elastic shear constant,  $c_s = (C_{11} - C_{12})/2$ , would vanish at a fractional volume of about 0.6.<sup>43</sup> A more detailed

calculation showed this to occur at 0.51.<sup>44</sup> The experimental value in all cases is about 0.54, which is reached when the pressure reaches about  $3.5B_0$ , where  $B_0$  is the bulk modulus at zero pressure.

CsI has a second transition at 56 GPa, which is an orthorhombic distortion of the tetragonal phase.<sup>37,39</sup> The crystal structure is based on a simple orthorhombic lattice with a basis of Cs at 000 and I at  $1/2, 1/2, 1/2$ . It is interesting to note that this structure has essentially CN = 10 with 8 unlike nearest neighbors and two like neighbors at nearly the same distance. Thus in CsI, via two transitions, the coordination number increases from 8 to 10 and presumably at still higher pressures may go to CN = 12 in the metallic state.

**Note Added in Proof:** Recently, a collimated X-ray beam of 5- $\mu$ m diameter has been used to study X-ray diffraction at 2.55 Mbar and to obtain detailed pressure profiles across the diamond tip.<sup>45</sup> We believe these are the highest static pressures attained and measured in a diamond anvil cell.

*We acknowledge the National Science Foundation for support of this work under Grant DMR 86-12289.*

(36) Huang, T.-L.; Ruoff, A. L. *Phys. Rev. B* 1984, 29, 1112.

(37) Asaumi, K. *Phys. Rev. B* 1984, 29, 1118.

(38) Knittle, E.; Jeanloz, R. *Science (Washington, D.C.)* 1984, 223, 53.

(39) Vohra, Y. K.; Brister, K. E.; Weir, S. T.; Duclos, S. J.; Ruoff, A. L. *Science (Washington, D.C.)* 1986, 231, 1136.

(40) Brister, K. E.; Vohra, Y. K.; Ruoff, A. L. *Phys. Rev. B* 1985, 31, 4657.

(41) Huang, T.-L.; Brister, K. E.; Ruoff, A. L. *Phys. Rev. B* 1984, 30, 2968.

(42) Knittle, E.; Rudy, A.; Jeanloz, R. *Phys. Rev. B* 1985, 31, 588.

(43) Anderson, O. L.; Liebermann, R. C. *Phys. Earth Planet. Inter.* (1970), 3, 61.

(44) Vohra, Y. K.; Duclos, S. J.; Ruoff, A. L. *Phys. Rev. Lett.* 1987, 54, 570.

(45) Vohra, Y. K.; Duclos, S. J.; Brister, K. E.; Ruoff, A. L. Cornell Materials Science Center Report 6399, Cornell University, Ithaca, NY, March 1988.